Polymer Journal, Vol. 39, No. 11, pp. 1105–1111 (2007)

SPECIAL ISSUES -PROGRESS IN STRUCTURE ANALYSES OF POLYMERIC MATERIALS BY SYNCHROTRON RADIATION AND NEUTRON BEAM-

A Neutron Reflectivity Study on a Terraced Lamellar Morphology in a Block Copolymer Thin Film

Ken-ichi NIIHARA,[1] Ukyo MATSUWAKI,[1] Naoya TORIKAI,[2] Kotaro SATOH,[3] Masami KAMIGAITO,[3] and Hiroshi JINNAI[1,†]

[1]*Department of Macromolecular Science and Engineering, Graduate School of Science and Engineering, Kyoto Institute of Technology, Matsugasaki, Sakyo-ku, Kyoto 606-8585, Japan*
[2]*Neutron Science Laboratory, High Energy Accelerator Research Organization, 1-1 Oho, Tsukuba 305-0801, Japan*
[3]*Department of Applied Chemistry, Graduate School of Engineering, Nagoya University, Furo-cho, Chikusa-ku, Nagoya 464-8603, Japan*

(Received July 17, 2007; Accepted July 24, 2007; Published September 14, 2007)

ABSTRACT: A microphase-separated structure of a poly(deuterated styrene-*block*-2-vinylpyridine) (dPS-*b*-P2VP) block copolymer thin film was studied by neutron reflectivity (NR). The spun-coated dPS-*b*-P2VP block copolymer (on a Si substrate) showed the coexistence of a minority thin lamellar layer (holes) dispersed in a majority thick layer. The "terraced structure" was formed due to the mismatch between the initial film thickness and the intrinsic lamellar periodicity of the dPS-*b*-P2VP block copolymer. The amount and height of the holes were evaluated using atomic force microscopy (AFM), transmission electron microscopy (TEM) and transmission electron microtomography (TEMT). The three-dimensional (3D) images obtained from the TEMT experiments clearly showed that the microphase-separated structure inside the thin film was homeotropically aligned. The thickness of the thick and the thin lamellar layers corresponded to $(5/2)L_0$ and $(3/2)L_0$, respectively (L_0 is the lamella periodicity in the bulk state). The NR profile from the dPS-*b*-P2VP thin film, R_{exp}, showed many distinctive scattering peaks. Based on the structural information obtained from the microscopy, a scattering length density profile along the depth direction, *i.e.*, the direction normal to the film surface, b/v_{TEMT}, was evaluated, which was then used as an initial profile in the conventional model fitting method. An excellent best-fit to R_{exp} was obtained using b/v_{TEMT}, even though the thin film had the terraced structure. The surface coverage of the holes was estimated from the resulting b/v, which was in good agreement with the estimated value from TEM. [doi:10.1295/polymj.PJ2007100]

KEY WORDS Block Copolymer / Thin Film(s) / Transmission Electron Microtomography / Neutron Reflectivity /

In recent years, block copolymer thin films have drawn considerable attention in many technological areas such as microelectronics[1–4] and nanoporous films.[5,6] For example, Guarini *et al.* reported that block copolymer thin films can be used as the mask layers for dense nanoscale dot patterning.[1] They also presented the following possible applications of the nanometer-scale structures: high surface area substrates for capacitors and biochips, quantum dot arrays for nonvolatile memories, silicon pillar arrays for vertical transistors or field-emission displays, etc. In order to understand the self-assembling morphologies of the block copolymer thin films, it is particularly important to study in detail the self-assembling processes and the resulting morphologies.

The surface interaction (between the block copolymer and substrate or between the block copolymer and air surface) as well as the confinement significantly affects the microphase-separated structures.[7,8] In order to obtain a smooth surface, *i.e.*, constant thickness in the block copolymer thin film, the film thickness, T, should fulfill the following relationship (in the case of an asymmetric wetting condition):

$$T = (n + 1/2)L_0, \tag{1}$$

where n and L_0 are an integer number and the domain periodicity of the microphase-separated structure, respectively. For films with thicknesses which do not initially satisfy the requirement, islands or holes with a step height of L_0 are formed on the surface ("terraced" or "holes" structure).[7,9,10]

The organization of a poly(deuterated styrene-*block*-methyl methacrylate) block copolymer thin film on silicon has been studied previously by Mayes *et al.* by neutron and X-ray reflectivity.[11] Their work suggests that, after substantial annealing time, surface roughnesses decay or grow into holes depending on the initial film thickness. Although the reflectivity

†To whom correspondence should be addressed (E-mail: hjinnai@kit.ac.jp).

profiles (corresponding to the terraced structure) were carefully analyzed, the scattering length density profiles were not comprehensively explained except for the decrease in the surface dPS-rich half-layer and the simultaneous increase in the total film thicknesses. Based on these two trends, Mayes *et al.* concluded that holes formed in their thin film. Cai *et al.* later challenged the terraced structure in a poly(styrene-*block*-methyl methacrylate) block copolymer thin film. They measured the surface structure in real-space by atomic force and optical microscopies, which was compared with the results from the reciprocal space, *i.e.*, specular and off-specular reflectivity profiles.[12] The height of the holes determined from the scattering and microscopic methods agreed well, although the internal morphology in the thin film was only assumed and left unclear. Thus, even though the reflectivity measurement is a very powerful technique, it always involves some kinds of assumption(s) due to the lack of complete real-space structural information.

In the present paper, we employ transmission electron microscopy (TEM) and transmission electron microtomography (TEMT) to image not only the surface but also the internal morphologies. Surface morphology will also be examined by atomic force microscopy (AFM). With the three-dimensional (3D) structural information obtainable by these three real-space methods, the scattering length density profiles with truly physical meaning (not merely an assumption!) will be obtained, which will be further used to explain the neutron reflectivity (NR) profiles for better statistical accuracy in understanding the terraced structures.

EXPERIMENTAL

Materials

The poly(deuterated styrene-*block*-2-vinylpyridine)(dPS-*b*-P2VP) block copolymer was purchased from Polymer Source Inc., Canada. The number-average molecular weights, M_n, of the dPS and P2VP blocks were 55,000 and 38,000, respectively, which were measured by ^{1}H nuclear magnetic resonance and elemental analysis, in order to determine the exact volume fractions of the dPS and P2VP blocks. The polydispersity index, M_w/M_n, is 1.15. The volume fraction of dPS is 0.59. The scattering length density, b/v, of the dPS and P2VP blocks were $6.47 \times 10^{-4}\,nm^{-2}$ and $1.95 \times 10^{-4}\,nm^{-2}$, respectively.

Specimens

In order to observe the morphology in the bulk state of the dPS-*b*-P2VP block copolymer, a film specimen was prepared by solvent casting from a 5 wt % 1, 4-dioxane solution for *ca.* one week. The cast film was annealed at 170 °C for one day under vacuum. The annealed film was then ultramicrotomed using a diamond knife at room temperature with a Lica Ultracut UCT. The ultrathin section was transferred onto a Cu mesh grid with a polyvinylformal substrate. Prior to the transmission electron microscope (TEM) observations, the ultrashin section was stained with I_2 vapor for 3 h. The morphology in the bulk state was observed by TEM, before the NR and TEMT experiments. We confirmed that this copolymer formed a typical lamella morphology in the bulk state. The domain periodicity of lamella morphology, L_0, was evaluated to be 70 *nm* from the TEM micrograph.

The block copolymer thin film was prepared by spin-coating from a 2 wt % 1, 4-dioxane solution onto a silicon (Si) substrate at 900 rpm. The thin film was annealed at 170 °C for 14 d under vacuum. The same thin film was used in the microscopy and reflectivity experiments.

Atomic Force Microscopy

The free surface structure of the annealed thin film was observed by atomic force microscopy (AFM) (MFP-3D-SA, Asylum Technology Co., Ltd. U.S.A.) operated in the tapping mode using a silicon tip. The amount and the height of the holes were measured from the AFM height images.

Transmission Electron Microscopy and Transmission Electron Microtomography

The portion of the dPS-*b*-P2VP thin films used later in the NR experiments was made into a TEM specimens. In order to observe the thin film from the top-view, the thin film was peeled off the Si substrate onto a pool of hydrofluoric acid. The floating thin film on hydrofluoric acid was picked up by Cu mesh grids for the TEM experiment. In order to observe the thin film from a cross-sectional view, the thin film was stained with I_2 vapor for 3 h and subsequently coated with carbon in order to reduce the charge and to enhance the heat transfer during the ultra-thin sectioning using the focused-ion-beam (FIB) method (JEM-9310FIB, JEOL Co., Ltd., Japan).[13] We note here that the sectioning without peeling the block copolymer thin film off the Si substrate became possible by using FIB. The section was put on the Cu mesh grid for TEM and TEMT experiments. Prior to TEMT observations, the gold particles (diameter: 10 *nm*) were placed on the ultrathin sections using the gold colloidal solution (GCN005, BBInternational Co. Ltd., U.K.).

The TEM and TEMT observations were carried out using a JEM-2200FS (JEOL Co., Ltd., Japan) operated at 200 kV and equipped with a slow-scan CCD camera (Gatan USC1000, Gatan Inc., USA) as a de-

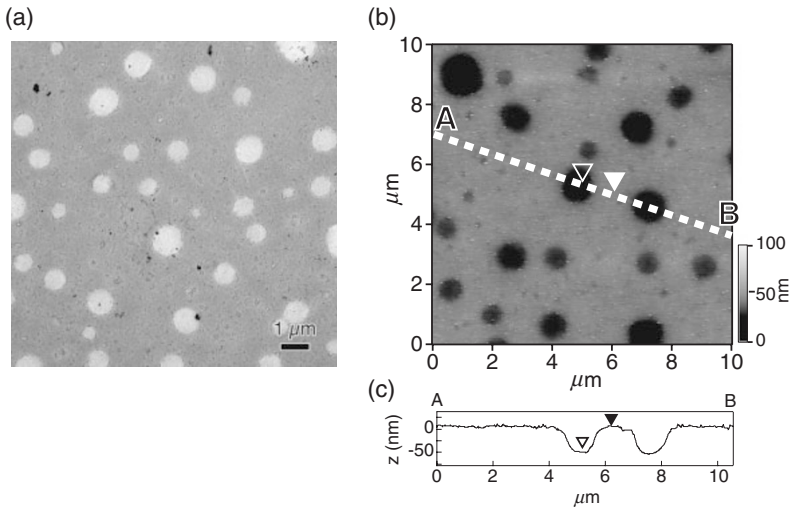

Figure 1. (a) TEM micrograph of the dPS-*b*-P2VP thin film. Because the thin film was not stained, the image contrast is proportional to the thickness of the film. Thus, the light-gray circular regions, holes, are thinner than their exterior. (b) AFM height image from the free surface of the dPS-*b*-P2VP thin film. The black region is lower than the gray area. (c) Cross-sectional height profile corresponding to the dashed line in part (b). The filled and an open triangles represent the same positions in parts (b) and (c). The depth of the holes, *i.e.*, the height difference between the two triangles, is *ca.* 66 *nm*.

tector.[14–20] Only the transmitted and elastically scattered electrons (electron energy loss of 0 ± 15 eV) were selected by the energy filter installed in the JEM-2200FS (Omega filter, JEOL Co., Ltd., Japan). Two series of TEM projections were acquired at tilt angles ranging from -56° to $+60^\circ$ and -47° to $+52^\circ$ in 1° increments, respectively. The two tilt series were then aligned by the fiducial marker method[21] using the Au particles and then reconstructed on the basis of the filtered back projection method.[22] Note that the mean alignment errors,[23] averaged over all of the fiducial markers used in the alignment, were respectively 0.58 *nm* and 0.49 *nm* which were less than the pixel resolution regardless of the tilt angles.[17] All alignment and reconstruction procedures were carried out using software developed in our laboratory.

Neutron Reflectivity

The annealed thin film, cut into a $7\,cm \times 4\,cm$ section from the spun-coated wafer, was used for the NR experiment, which was the same thin film used for AFM and TEMT experiments. The NR measurement was carried out using the PORE pulsed-neutron reflectometer[24] at the Neutron Science Laboratory, High Energy Accelerator Research Organization in Tsukuba. In this study we observed the specular reflection using white neutrons with a wavelength, λ, range of 0.3 to 1.6 *nm*. The incident angle, θ, was fixed at 0.4, 1.0, 2.0 deg, and the angular resolution, $\Delta\theta/\theta$, was kept at 5% by adjusting the width of the two incident slits. An algorithm of Parratt based on a recursive calculation method[10,25] was used to calculate the reflectivity profiles from the scattering length density (b/v) profile along the direction perpendicular to the film surface, *i.e.*, along the Z-direction. χ^2 of the fitting error between the measured and calculated reflectivities was calculated by,

$$\chi^2 = \frac{1}{1-N}\sum_{i=1}^{N}\left(\frac{R_{m,i}-R_{c,i}}{R_{m,i}}\right)^2 \qquad (2)$$

where $R_{m,i}$ and $R_{c,i}$ are the measured and calculated reflectivities at a specific scattering vector, q_z ($q_z \equiv (4\pi/\lambda)\sin\theta$), respectively. N is the total number of measured points. On that fitting protocol, χ^2 was calculated to be as low as possible. A software available on the web, Parratt32 (http://www.hmi.de/), was used in the fitting protocol.

RESULTS

A terraced structure in a dPS-b-P2VP block copolymer thin film

Figure 1(a) shows a TEM micrograph of a dPS-*b*-P2VP block copolymer thin film. Because the thin film was not stained and thus the lamellar structure in the film cannot be seen under TEM, the image contrast of the TEM image directly corresponds to the thickness of the film. Therefore, the white regions in the picture are thinner than the gray region. Many such white circles are observed in Figure 1(a), implying that the block copolymer thin film exhibited "holes". In order to measure the depth of the holes structure, the free surface of the thin film was examined by AFM, the result of which is shown in Figure 1(b). Figure 1(c) demonstrates the measured height along the dashed line in part (b). The average depth of the terraces, *ca.* 66 *nm*, was in good agreement with the lamellar periodicity, L_0, measured in

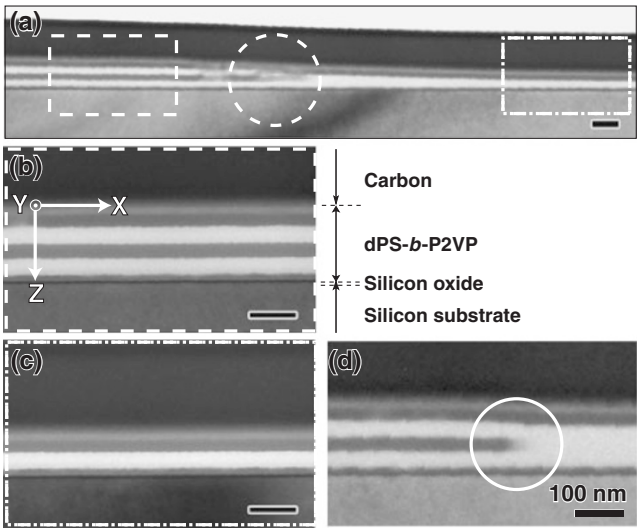

Figure 2. Cross-sectional TEM micrographs of the dPS-*b*-P2VP thin film. The dark and bright phases are the I_2-stained P2VP and dPS microdomains, respectively. Part (a) shows the overall low-magnified image. There are two terraces with different thicknesses. The thicker one (dashed rectangle) is $(5/2)L_0$ thick, while the thinner one (dot-dashed rectangle) is $(3/2)L_0$ (L_0 is the lamellar periodicity). They are shown with higher magnification in parts (b) and (c), respectively. The *Z*-axis is the direction normal to the film surface. The dashed white circle in part (a) indicates the dislocation of the P2VP microdomain, which is magnified in part (d) (white circle).

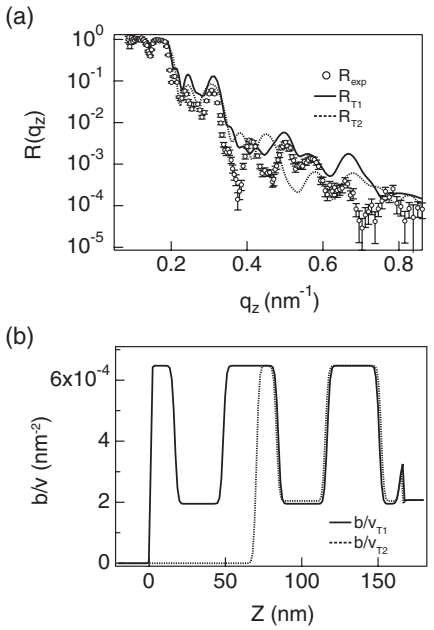

Figure 3. (a) NR profile of the dPS-*b*-P2VP thin film (open circles). The lines are the calculated NR profiles based on the scattering length density profile, b/v, obtained from the TEMT image. The solid and dashed lines are NR profiles based on b/v of the thick terrace (solid line in part (b)) and the thin terrace (dashed line in part (b)), respectively. TEMT results are used to estimate the b/v of each terrace.

the bulk, *i.e.*, 70 *nm*. Thus, we speculate, at this stage, that the terraces had one domain periodicity thinner than the majority thick region. The surface coverage of the terraces at the film surface was estimated to be *ca.* 25% from the TEM images (total measured area for the measurement: *ca.* $100 \times 100\,\mu m^2$). Because the lamellar layers were parallel to the substrate [see later in Figure 2], neither TEM (projection) nor AFM (surface image) can capture the microphase-separated structure.

In order to observe lamellae in the thin film, cross-sectional TEM micrographs were obtained as shown in Figure 2. Note that the cross-sectional section (specimen) for the TEM and the TEMT experiments was prepared by FIB from exactly the same spun-cast film used later in the NR experiment. The *Z*-direction corresponds to the direction along the depth of the dPS-*b*-P2VP thin film. Dark and white phases correspond to I_2-stained P2VP and the dPS domain, respectively. The dPS-*b*-P2VP thin film formed an alternating lamella morphology aligned parallel to the film surface. The substrate and the free surface of the thin film were wetted by the P2VP and dPS, respectively, *i.e.*, an asymmetrical wetting case. There were two regions in the picture: the thicker [a dashed rectangle in Figure 2(a) and 2(b)] and thinner [a dotted-dashed rectangle in Figure 2(a) and 2(c)] regions. The thickness of the former corresponded to $(5/2)L_0$, while that of the latter was $(3/2)L_0$. Needless to say, the thinner part is the hole. We hereafter call the thick and thin part of the dPS-*b*-P2VP block copolymer thin film T1 and T2, respectively. As mentioned in Figure 1, T1 is thicker than T2 by *ca.* 70 *nm* that agreed with the periodicity of the lamellar morphology. The thickness of the terrace is quantized as predicted by eq 1. Note that the depth of the hole evaluated from the TEM micrograph in Figure 2, is in excellent agreement with that obtained from AFM [see Figure 1]. In addition, the dislocations of the dPS and P2VP microdomains, *i.e.*, the discontinuous lamella layer at the edge of the terraces, have been observed in the boundary between T1 and T2 [see a dashed white circle in Figure 2(a) and a white circle in Figure 2(d), respectively].

Structural analysis of terraced structure of dPS-b-P2VP block copolymer thin film

The neutron reflectivity measurements have been carried out in order to statistically evaluate the internal morphology of the dPS-*b*-P2VP block copolymer thin film. Figure 3 displays the measured NR profile, R_{exp}, in which the reflectivity, R, is plotted against the magnitude of the scattering vector along the *Z*-direction, q_z. R_{exp} decreased with increasing q_z with

many scattering peaks that indicate highly-ordered structures inside the thin film. In the conventional model fitting method to analyze the NR profile, one needs the initial scattering density profile, b/v, as a first "guess". The precision of the fitting and hence the conclusions drawn from the analysis heavily depend on the initial density profile; a dissimilar b/v could sometimes fit an NR profile with similar precision. In other words, the analysis could be heavily model-dependent, and the uniqueness of the resulting b/v has to be carefully examined.[8] Combining real space structural information with the fitting method is therefore an effective strategy to reduce such uncertainty in the fitting protocol.

As the real-space observation technique, TEM may be the most common choice. However, making ultrathin films for the cross-sectional TEM is rather difficult because one needs to cut the substrate together with the thin film. In many cases, the substrate is made of Si (as in this study) so that it cannot be easily microtomed. One needs to either peel the thin film off the substrate or to find a way to cut the hard substrate. Because the structural change during the peeling may cause a problem in the former, we used FIB to make the ultra thin section in this study. Note that it is possible to cut the Si substrate with FIB without damaging the block copolymer thin film if an appropriate treatment of the sample was done prior to the fabrication.[13] Even with the FIB sampling, however, it was found in our previous study that the cross-sectional TEM image of the thin film may not be sufficient to estimate the b/v due to (i) possible tilt of the section with respect to normal of the substrate, *i.e.*, the Z-axis, and (ii) overlapping the structure along the Y-axis[8] in the TEM micrograph. It is best to use TEMT to take a 3D image of the cross-sectional section and correct the tilt, if any, to evaluate truly vertical at the planes of the block copolymer thin film.

For the 3D reconstruction, the cross-sectional section of the thin film was tilted under TEM to take a series of projections, where the tilt axis was parallel to the X-direction in Figure 2. A 3D image of the dPS-*b*-P2VP thin film was obtained (not shown here) that clearly showed the lamellar morphology. The volume fraction of the dPS nanodomain was determined to be 0.60 from the 3D reconstruction. This volume fraction was in excellent agreement with the known composition of the copolymer, *i.e.*, 0.59.

The concentration profiles of the dPS block were estimated from the 3D image in the same way as in our previous study,[8] which were then converted to the scattering length densities, b/v. The b/v of the T1 and T2 regions b/v_{T1} and b/v_{T2} are shown by a solid line and a dashed line in Figure 3(b), respectively. The NR profiles based on these b/v_{T1} and b/v_{T2},

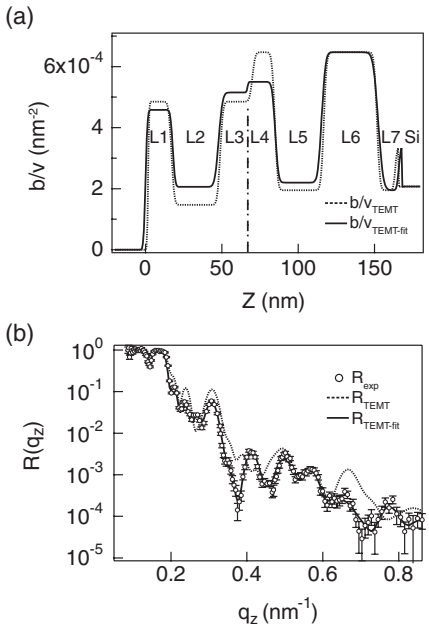

Figure 4. (a) Scattering length density profile, b/v, of the dPS-*b*-P2VP block copolymer thin film. The dashed line shows an estimated scattering length density profile, b/v_{TEMT}, used for an initial model for the conventional fitting protocol.[25] The model was constructed by combining the b/v value of the two terraces (see Figure 3) on the basis of the coverage of the thin terrace (holes), *i.e.*, 25%. The coverage was determined using AFM, TEM and TEMT. The best-fit scattering density profile, $b/v_{TEMT\text{-}fit}$, is shown by the solid line. (b) NR profile of the dPS-*b*-P2VP thin film, R_{exp} (open circles). The dashed and solid lines are the NR profiles calculated from b/v_{TEMT} and $b/v_{TEMT\text{-}fit}$, respectively. χ^2 calculated from equation (2) was 4.57×10^{-2}.

R_{T1} and R_{T2}, were obtained from the TEMT experiments and are shown by the solid line and the dashed line in Figure 3(a). R_{T1} reproduced R_{exp} better than R_{T2} did, indicating that the thick terrace corresponding to the thickness of $(5/2)L_0$ was the major structure in the dPS-*b*-P2VP thin film. There is, however, a distinct deviation in R_{T1} from R_{exp} probably because of the indispensable contribution of R_{T2} to R_{exp}. In order to create a better initial scattering length density profile for the dPS-*b*-P2VP block copolymer thin film, b/v_{T1} and b/v_{T2} were combined based on the coverage of the holes estimated in Figure 1, *i.e.*, 25%. The combined scattering length density profile, b/v_{TEMT}, is shown by a dashed line in Figure 4(a). The corresponding NR profile, R_{TEMT}, is demonstrated also by a dashed line in Figure 4(b). R_{TEMT} reproduced R_{exp} very well, much better than R_{T1} did. In other words, TEMT already provided a reasonable initial model to describe the NR profile with good statistics.

The b/v_{TEMT} was subsequently used as the initial guess in the model fitting method.[25] The resulting best-fit scattering density profile, $b/v_{TEMT\text{-}fit}$, and the corresponding reflectivity profile, $R_{TEMT\text{-}fit}$, are shown

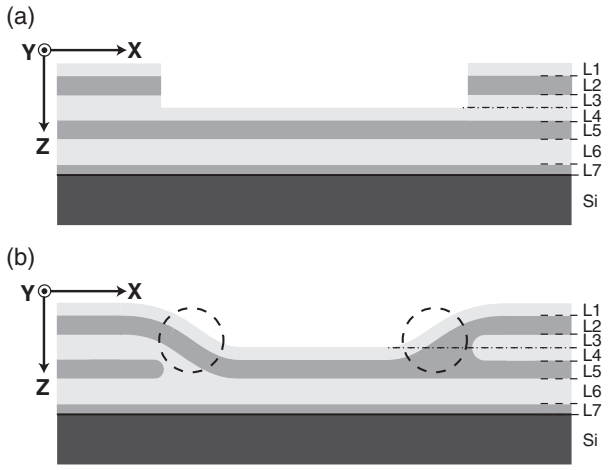

Figure 5. Schematic cross-sectional models of the terraced structure of the dPS-*b*-P2VP thin film on the Si substrate. The light gray and the gray layers are the dPS and P2VP layer, respectively. (a) A simplified mode where the lamellar structures are discontinuous between the terrace boundary. (b) A proposed model based on the TEM and TEMT observations. The lamellar layers are continuous at the terrace boundary through the homogeneously aligned lamellae.

by the solid lines in Figure 4(a) and 4(b), respectively. $R_{TEMT\text{-}fit}$ showed excellent agreement with R_{exp} over the entire range of q_z. It is essential to point out that the $b/v_{TEMT\text{-}fit}$ has strong support from the real-space data, *i.e.* the TEMT image in this case.

DISCUSSION

Let us now discuss $b/v_{TEMT\text{-}fit}$ in terms of real space information obtained from TEM, TEMT and AFM. Figure 5(a) shows a simplified model of the terraced structure where two terraces with different thicknesses are displayed. The thicker and thinner terraces of the structure corresponded to $(5/2)L_0$ and $(3/2)L_0$, respectively. We call the latter a "hole" throughout this paper. The thicknesses of the terraces were *directly* measured by AFM and TEM. The scattering length density profile shown by the dashed line in Figure 4(a) was based on the above simplified model. Namely, the terraces are composed of homeotropically aligned lamellae and the step between them contains dislocation. The coverage of the holes was set to 25%. According to Carvalho and Thomas,[26] however, the steps contained homogeneously aligned lamellae and a minimal surface may be a good model at the step.

Although the detailed morphology at the boundary region between the terraces is still not known, the actual morphology at the step will not be as simple as the dislocation as shown in Figure 5(a) because the system tries to minimize the surface free energy by generating complicated 3D morphology there. A more realistic step morphology observed from TEM and TEMT is modeled and displayed in Figure 5(b). In Figure 5, both dPS (light gray) and P2VP (gray) layers are displayed with numbers from the air surface. For example, L1 is the closest dPS layer from the air surface that corresponds to the first peak in b/v shown in Figure 4(a) (also labeled L1). We note here that the model shown in Figure 5(b) may not be quite accurate at the boundary because the step morphology may be three-dimensionally complicated along the *Y*-axis. In other words, the color at the step morphology marked by the dashed circles in Figure 5(b) may not be the same gray level as that of pure dPS nor P2VP. In order to have even more accurate model, detailed 3D observations using TEMT are necessary to unveil the step morphologies, which is in progress.

From the schematic, it is obvious that the L1 (and L2, L3) layer represents only a thicker terrace, while the deeper layers, *i.e.*, L4 and L5, contain structural information from both terraces. The scattering length density, $b/v_{TEMT\text{-}fit}$, of L1 after the fitting was $4.58 \times 10^{-4}\,nm^{-2}$, which is 71% of a pure dPS layer, $6.47 \times 10^{-4}\,nm^{-2}$. Therefore, the coverage of holes was determined to be 29%, in agreement with the estimated value from TEM, *i.e.*, 25%.

The L2 and L3 layers may be affected by the boundary morphology at the step. The $b/v_{TEMT\text{-}fit}$ value of the L2 and L3 layers were $2.06 \times 10^{-4}\,nm^{-2}$ and $5.15 \times 10^{-4}\,nm^{-2}$, respectively. These values are larger than those in the simplified model shown in Figure 5(a) than the actual coverage, 29%. Note that as the coverage of the holes becomes larger in the simplified model, the scattering length density of L2 and L3 becomes smaller. Thus, if the simplified model were true, L2 and L3 of $b/v_{TEMT\text{-}fit}$ (solid line, the coverage of the hole: 29%) would be smaller than those of b/v_{TEMT} (dashed line, the coverage of the hole: 25%), which is apparently not the case. In reality, the free surface of the dPS-*b*-P2VP thin film was wetted by the dPS block as shown in Figure 5(b), and the lamellar morphology was continuous throughout the terrace boundary.[27] It is speculated that the surface-wetting dPS layer contributed to the L2 and L3 layers that increased b/v at these depths. b/v at deeper levels, L4 and L5, may also be affected by the presence of the terrace boundary, and this is probably the reason why $b/v_{TEMT\text{-}fit}$ deviated from the predicted scattering length profile. In order to fully understand $b/v_{TEMT\text{-}fit}$, it is necessary to observe the terrace boundary in more detail in 3D. Such experiments are in progress.

Acknowledgment. The authors are grateful to NEDO for supporting this study through a Japanese National Project "Nano Structured Polymer Project"

by the Ministry of Economy, Trade and Industry. This work is partially supported from the Ministry of Education, Science, Sports and Culture through Grants-in-Aid No. 1855019 and No. 19031016. The authors are grateful to Mr. H. Atarashi and Prof. K. Tanaka of Kyushu Univ. for their valuable discussion and comments. We also thank Dr. J. Benkoski, Dr. B. C. Berry, Dr. R. L. Jones and Dr. A. Karim of the National Institute of Standards and Technology, US, for assistance with the AFM measurements and their valuable comments.

REFERENCES

1. K. W. Guarini, C. T. Black, Y. Zhang, H. Kim, E. M. Sikorski, and I. V. Babich, *J. Vac. Sci. Technol., B*, **20**, 2788 (2002).
2. I. W. Hamley, *Nanotechnology*, **14**, R39 (2003).
3. C. Park, J. Yoon, and E. L. Thomas, *Polymer*, **44**, 6725 (2003).
4. M. P. Stoykovich, M. Müller, S. Kim, H. H. Solak, E. W. Edwards, J. J. Pablo, and P. F. Nealey, *Science*, **308**, 1442 (2005).
5. G. Widawski, M. Rawiso, and B. François, *Nature*, **369**, 387 (1994).
6. E. M. Freer, L. E. Krupp, W. D. Hinsberg, P. M. Rice, J. L. Hedrick, J. N. Cha, R. D. Miller, and H. Kim, *Nano Lett.*, **5**, 2014 (2005).
7. M. J. Fasolka and A. M. Mayes, *Ann. Rev. Mater. Sci.*, **31**, 323 (2001).
8. K. Niihara, U. Matsuwaki, N. Torikai, H. Atarashi, K. Tanaka, and H. Jinnai, *Macromolecules*, in press.
9. R. J. Spontak and N. P. Patel, in "Developments in BLOCK COPOLYMER Science and Technology", I. W. Hamley Ed., John Wiley & Sons, Chichester, New York, 2004, pp 91–115.
10. T. P. Russell, *Mater. Sci. Rep.*, **5**, 171 (1990).
11. A. M. Mayes, T. P. Russell, P. Bassereau, S. M. Baker, and G. S. Smith, *Macromolecules*, **27**, 749 (1994).
12. Z. Cai, K. Huang, P. A. Montano, T. P. Russell, J. M. Bai, and G. W. Zajac, *J. Chem. Phys.*, **93**, 2376 (1993).
13. K. Niihara, T. Kaneko, T. Suzuki, Y. Sato, H. Nishioka, Y. Nishikawa, T. Nishi, and H. Jinnai, *Macromolecules*, **38**, 3048 (2005).
14. K. Niihara, Y. Nishikawa, T. Nishi, and H. Jinnai, *Trans. Mater. Res. Soc., Jpn.*, **30**, 617 (2005).
15. H. Jinnai, K. Sawa, and T. Nishi, *Macromolecules*, **39**, 5815 (2006).
16. T. Kaneko, K. Suda, K. Satoh, M. Kamigaito, T. Kato, T. Ono, E. Nakamura, T. Nishi, and H. Jinnai, *Macromol. Symp.*, **242**, 80 (2006).
17. T. Kaneko, H. Nishioka, T. Nishi, and H. Jinnai, *J. Electron. Microsc.*, **54**, 437 (2005).
18. N. Kawase, M. Kato, H. Nishioka, and H. Jinnai, *Ultramicroscopy*, **107**, 8 (2007).
19. H. Jinnai, K. Yasuda, and T. Nishi, *Macromol. Symp.*, **245–246**, 170 (2006).
20. H. Sugimori, T. Nishi, and H. Jinnai, *Macromolecules*, **38**, 10226 (2005).
21. P. K. Luther, M. C. Lawrence, and R. A. Crowther, *Ultramicroscopy*, **24**, 7 (1988).
22. R. A. Crowther, D. J. DeRosier, and A. Klug, *Proc. R. Soc. London*, **A 317**, 319 (1970).
23. R. J. Spontak, J. C. Fung, M. B. Braunfeld, J. W. Sedat, D. A. Agard, L. Kane, S. D. Smith, M. M. Satkowski, A. Ashraf, D. A. Hadjuk, and S. M. Gruner, *Macromolecules*, **29**, 4494 (1996).
24. M. Takeda and Y. Endoh, *Physica B*, **267–268**, 185 (1999).
25. L. G. Parratt, *Phys. Rev.*, **95**, 359 (1954).
26. B. L. Carvalho and E. L. Thomas, *Phys. Rev. Lett.*, **73**, 3321 (1994).
27. Y. Liu, M. H. Rfailovich, J. Sokolov, S. A. Schwarz, and S. Bahal, *Macromolecules*, **29**, 899 (1996).